INSTYTUT PROBLEMÓW JĄDROWYCH
im. ANDRZEJA SOŁTANA
SOLTAN INSTITUTE FOR NUCLEAR STUDIES

LIBRA

RAPORT SINS - 9/ VI

TESTS OF MODELS FOR EXCLUSIVE ρ^0 PRODUCTION IN DEEP INELASTIC MUON SCATTERING

ANDRZEJ SANDACZ

Soltan Institute for Nuclear Studies,
Hoża 69, 00-681 Warszawa, Poland

NAME	ID No	M.S.
WOLBERS	6807	120

RETURN TO FERMILAB

OTWOCK - ŚWIERK 1995

Andrzej Sandacz: Tests of Models for Exclusive ρ^0 Production in Deep Inelastic Muon Scattering. The data on exclusive ρ^0 production in deep inelastic muon scattering are compared to selected models. The following models are considered: the model of exchange of two non-perturbative gluons, the colour transparency model, the Glauber model and the Vector Meson Dominance model.

Andrzej Sandacz: Testowanie modeli opisujących ekskluzywną produkcję mezonów ρ^0 w głęboko-nieelastycznym rozpraszaniu mionów. Dane doświadczalne dotyczące ekskluzywnej produkcji mezonów ρ^0 w głęboko-nieelastycznym rozpraszaniu mionów są porównane z wybranymi modelami. Rozpatrywane są następujące modele: model wymiany dwóch nieperturbacyjnych gluonów, model kolorowej przezroczystości, model Glaubera i model dominacji mezonów wektorowych.

Wydaje Instytut Energii Atomowej - OINTEA
Nakład: 60 egz. Objętość: ark.wyd.0,7; ark.druk.1,5.
Data złożenia maszynopisu: 10.04.1995. Pr.3158 z dnia 1993.01.04.

In this paper we compare the data on exclusive ρ^0 muoproduction at large photon virtuality Q^2 with selected theoretical models. The exclusive ρ^0 production reaction is

$$\mu + N \rightarrow \mu + N + \rho^0, \tag{1}$$

in which the only particle produced is ρ^0. This reaction can be described in terms of the virtual photoproduction process $\gamma^* N \rightarrow \rho^0 N$. To facilitate comparison of the data from different nuclear targets, the presented cross sections will be given per nucleon.

The paper consists of two parts. In the first part we compare the data from elementary targets (hydrogen and deuterium) with predictions of a group of models which assume an exchange of a pair of non-perturbative gluons. In the second part we compare the data from nuclear targets with predictions of the colour transparency model and with the Glauber-VMD model.

As an introduction we give a brief review of models describing diffractive vector meson production in deep inelastic scattering.

1. Introduction

There is a widespread theoretical belief that the exclusive leptoproduction of vector mesons ($\rho^0, \omega, \phi, J/\psi, \Upsilon$) is predominantly a diffractive process, even at large Q^2. It is supported by the low Q^2 (< 2 GeV^2) data on the production of light vector mesons [1], which are in a reasonable agreement with the Vector Meson Dominance (VMD) model. At large Q^2 the data are less numerous. For exclusive ρ^0 production they come from the experiments of EMC [2,3], NMC [4,5], E665 [6] and ZEUS [7].

The first proposed model for large Q^2 was that of Ref. [8], in which exclusive ρ^0 production is described assuming 'soft' pomeron exchange. The pomeron characteristics were determined phenomenologically from soft hadron processes and from deep inelastic scattering in the range of small values of the Bjorken scaling variable x, from which the cross sections for exclusive ρ^0 production were calculated without free parameters. Thus the studied process served as a consistency check of the model.

Other models were inspired by perturbative QCD [9-13]. These models have much in common. In the kinematical limits $Q^2 \gg m_V^2$ and $W^2 \gg Q^2 \gg -t$, where m_V is the vector meson mass, W is the total energy in the $\gamma^* N$ center of mass system and t the four momentum transfer squared to the recoil nucleon, these models describe the process as a product of the three amplitudes:

- the amplitude for the virtual photon to fluctuate into a quark-antiquark pair of a given flavour;
- the amplitude for the pair of quarks to interact with the nucleon by exchange of gluons;
- the amplitude for the scattered quark pair to combine into a vector meson.

The main differences between the models are due to the differences in the description of the intermediate state quark-antiquark pair in terms of constituent or

current quarks, in the choice of the vector meson wave functions, and in the treatment (or neglecting) of non-perturbative effects for gluons.

In the model of Donnachie and Landshoff [9] and in a version of this model by Cudell [10] the gluon propagator has a perturbative and a non-perturbative part. The latter depends on the gluon confinement length a, which was estimated from the analysis of the small x behaviour of the nucleon structure function and from the calculations of gluon condensates [9]. Non-perturbative effects are predicted to appreciably affect the Q^2 distribution at moderate Q^2 (several GeV^2 for ρ^0 production).

There is a remarkable similarity between most of the predictions of the phenomenological pomeron model of Ref. [8] and those of the QCD inspired models of Ref. [9,10], which include just the simplest two gluon exchange graphs. It is expected that including higher order graphs in the latter models may improve the agreement with the former model and could reproduce the Regge-type energy dependence predicted by the 'soft' pomeron model.

In another group of models the interaction of virtual quark-antiquark pair with the target nucleon is calculated using perturbative QCD [11-13]. These models predict that the forward ($t = 0$) cross section for exclusive vector meson production depends quadratically on the gluon structure function $\bar{x}G(\bar{x}, \bar{Q}^2)$. (Relations between the variables $\bar{x}$, $\bar{Q}^2$ and x, Q^2 depend on the model.) Thus, as suggested in Ref. [11], the data on exclusive vector meson production may allow a determination of the gluon distribution in the nucleon. Due to the quadratic dependence this process offers a higher sensitivity than the inelastic J/ψ production, as the cross section for the latter depends on $\bar{x}G(\bar{x}, \bar{Q}^2)$ linearly.

At large Q^2 both the wave function of the quark-antiquark fluctuation of the virtual photon and the cross section for such a colour dipole to scatter diffractively on a target are calculable. The transverse size r_Q of the dipole decreases with Q^2, whereas the cross section for the interaction of the dipole with a target is $\propto r_Q^2$ at small r_Q. Thus in the limit of $Q^2 \to \infty$ and $r_Q \to 0$ the cross sections vanish. This phenomenon is called colour transparency.

For elementary nucleon targets the above features enable the wave functions of the produced vector mesons to be probed by varying Q^2 [13,14]. For nuclear targets they lead to the prediction that the final state interaction between the produced quark-antiquark pair and the nucleus decreases with increasing Q^2 [12-14], and ultimately vanishes at very large Q^2 (colour transparency regime). Until this region is reached, the nuclear effects for exclusive vector meson production have, as pointed in Ref. 13, two origins: the final state interaction of the quark-antiquark pair with the nucleus and a possible change of the gluon distribution in the nuclear medium.

Despite the differences between the models of Ref. [9-13] (both non-perturbative and perturbative QCD), for the kinematical limits of large Q^2 and W they give qualitatively similar predictions. They predict asymptotic (in Q^2) behaviour of the type $1/Q^6$, linear growth with Q^2 of the ratio R ($= \sigma_L/\sigma_T$) of the cross sections for exclusive production by longitudinally and transversely polarised virtual photons, an approximate s-channel helicity conservation (SCHC) and a large fraction of longitudinally polarised vector mesons.

The energy dependence of the cross section is a sensitive test of the models. In

the energy range of the muon experiments ($W \sim 10 - 20$ GeV) all models predict a weak energy dependence, in agreement with the data. However, at the higher energies of the electron-proton collider at DESY ($W \sim 100$ GeV) there is an indication [7] that the cross section may grow faster than it is expected by the 'soft' pomeron model. In the perturbative QCD models of Ref. [11-13] this is related to the increase of the gluon structure function at small x.

2. The data from elementary targets

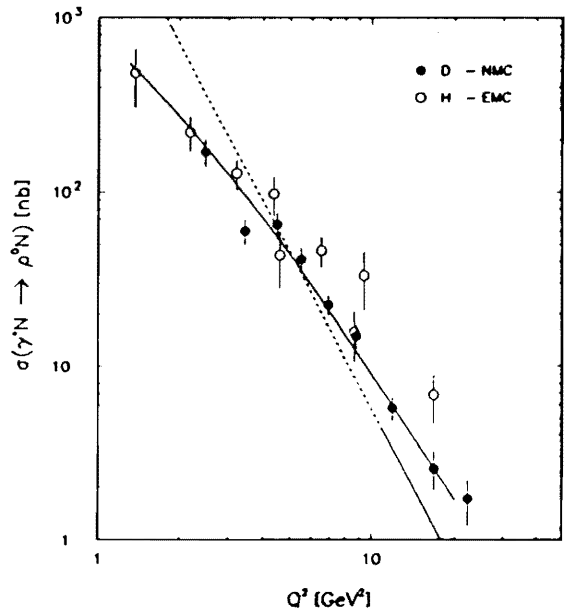

Figure 1: Exclusive ρ^0 virtual photoproduction cross section as a function of Q^2. The data are from the NMC experiment [4] for the deuteron (full symbols) and from the EMC [2] for the proton (open symbols). The solid curve represents the prediction of the model of Donnachie and Landshoff [15], in which exchange of two non-perturbative gluons is assumed. The dashed curve displays the asymptotic behaviour $\propto 1/Q^6$. The dashed curve was normalised to the measured cross section at $Q^2 = 6\,\mathrm{GeV}^2$.

In this section we compare the data on exclusive ρ^0 production from hydrogen and deuterium targets to the predictions of models which assume an exchange of a pair of two non-perturbative gluons [9,10]. The data are from the experiments of the EMC [2] and the NMC [4]. They include the cross sections for exclusive ρ^0 virtual photoproduction measured as a function of the variables Q^2 and ν (virtual photon energy in the laboratory system), the differential cross sections $d\sigma/dp_t^2$, where p_t^2 is the transverse momentum squared of the produced ρ^0 with respect to the direction of virtual photon, and the measured fractions of longitudinally polarised ρ^0 mesons. We discuss also the experimental determinations of the ratio R defined above.

In Fig. 1 the Q^2 dependence of the cross section for virtual photoproduction is shown. The NMC data for the deuteron are compared to the EMC data for the proton. Not shown are the systematic errors, which are about 20% for the NMC

data and 25% for the EMC. The measured cross sections in both experiments are compatible within the errors. As pointed out in Ref. [4] some small differences may be expected due to the different virtual photon polarisation in both experiments.

The solid curve represents the prediction of the model of Donnachie and Landshoff [15], in which the reaction proceeds through exchange of two non-perturbative gluons. The cross section for the process $\gamma^* N \rightarrow \rho^0 N$ in this model depends on the gluon confinement length a, the parameter which characterises the gluon propagator at large distances [9]. The solid curve in the Fig. 1 was calculated for the process $\gamma^* p \rightarrow \rho^0 p$ assuming the same virtual photon polarisation as in Ref. [2] and taking $a = (1.1\ \mathrm{GeV})^{-1}$, a value consistent with different theoretical estimates [9]. The dashed curve shows the $1/Q^6$ dependence predicted for asymptotic Q^2 by the QCD calculations [9-13]. This behaviour is different from the data. In the models of Refs. [9,10] the slower Q^2 dependence in the presently accessible Q^2 range is due to the non-perturbative part of the gluon propagator.

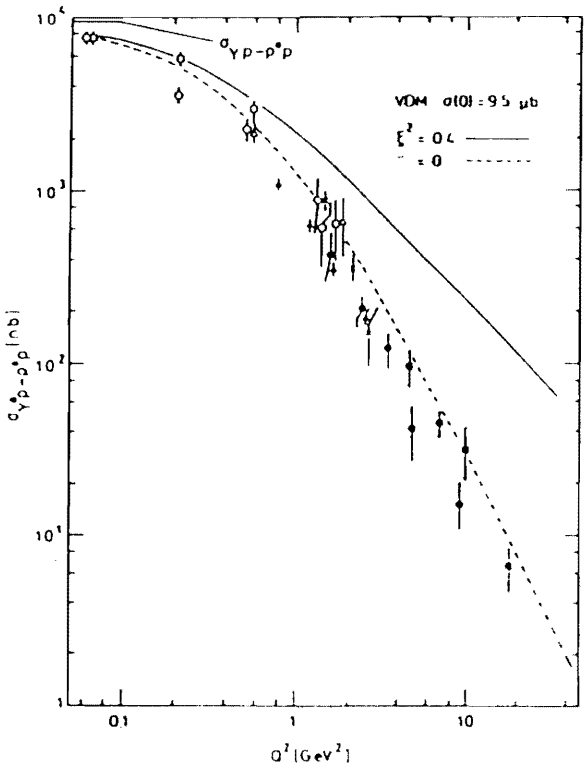

Figure 2: Exclusive ρ^0 virtual photoproduction cross section as a function of Q^2. The black circles and squares are the EMC data, the references to the data at lower Q^2 are given in [2]. The solid line is the VMD model prediction (2) with the parameter $\xi^2 = 0.4$. The dashed curve results if in equation (2) one assumes $\xi^2 = 0$.

It should be noted that at large Q^2 the Q^2 dependence of the virtual photoproduction cross section is at variance with the predictions of the classical VMD model, as already indicated in Ref. [2]. In this model the Q^2 dependence of the ρ^0 virtual photoproduction cross section can be written [1,16]

$$\sigma(Q^2) = \sigma(0)(1 + Q^2/m_\rho^2)^{-2}(1 + \epsilon\xi^2 Q^2/m_\rho^2), \qquad (2)$$

where $\sigma(0)$ is the cross section for real photoproduction and ϵ is the virtual photon polarisation. The term $\xi^2 Q^2/m_\rho^2$ is the ratio of the ρ^0 production cross section by longitudinal and transverse photons, i.e. R. Assuming s-channel helicity conservation, the parameter ξ^2 is related to the measured fraction of produced ρ^0 with helicity 0 (longitudinal polarisation) [2,4] (see also below). From the measured fraction one obtains $\xi^2 \simeq 0.4$. With this value the Q^2 dependence given by formula (2) is weaker than that observed in the data. This is illustrated in Fig. 2 taken from Ref. [2].

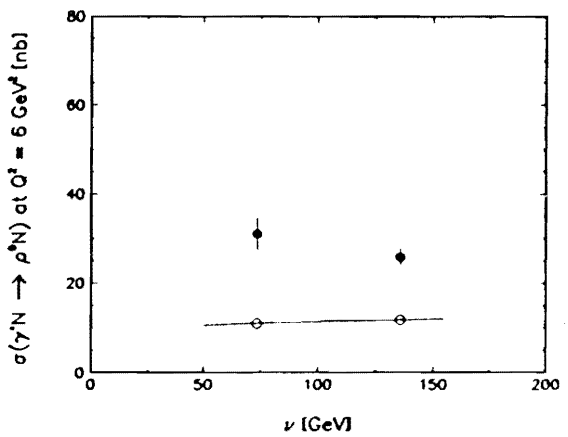

Figure 3: The ν dependence of exclusive ρ^0 virtual photoproduction cross sections for the deuteron at $Q^2 = 6$ GeV^2. Full symbols correspond to the measured total cross section, the open symbols to the cross section due to the transversely polarised photons. The curve displays the energy dependence expected for the pomeron exchange.

The ν dependence of the NMC data for the deuteron [4] is shown in Fig. 3. The cross sections are given at $Q^2 = 6$ GeV^2. The full symbols correspond to the total cross sections. There is no significant change of the cross section in the ν range 70 - 140 GeV.

Because the measured total cross section has contributions from virtual photons polarised transversely and longitudinally, its energy dependence is affected by the ν dependence of the ratio of the photon fluxes. Thus it is more straightforward to discuss separately the ν dependence of the cross sections of transverse and/or longitudinal photons. In Fig. 3 the transverse cross section, σ_T, is also shown (open symbols). It is calculated using the formula

$$\sigma = \sigma_T(1 + \epsilon R), \tag{3}$$

where σ is the measured total cross sections for exclusive ρ^0 production, $R = \sigma_L/\sigma_T$, and ϵ is the photon polarisation. The values of σ_T in Fig. 3 were obtained taking $R = 2.0$ [4].

The solid curve represents the ν dependence predicted by the 'soft' pomeron model. This behaviour is expected in certain models which assume a diffractive mechanism [8-10] and has the form $\sim (W^2/W_0^2)^\delta$, where $W^2 = M^2 + 2M\nu - Q^2$. The value of δ depends on the pomeron trajectory, $\alpha(t)$, and on the shape of the differential cross section $d\sigma/dp_t^2$. Using $\alpha(t) = 1.08 + 0.25t$ and the results of Ref.

[4] on $d\sigma/dp_t^2$ one obtains for the deuteron $\delta = 0.10$. A small increase of the cross section with ν predicted by the model is consistent with the data.

Fig. 4 shows the cross section $d\sigma/dp_t^2$ measured by the NMC for the deutron. The curve is the p_t^2 distribution predicted by the model of Ref. [10] for exclusive ρ^0 production on protons and renormalised to the deuteron data in the range $0.1 < p_t^2 < 1.0\ \mathrm{GeV}^2$, to exclude the influence of the coherent contribution. The incoherent part is fairly well described by the model up to $p_t^2 \sim 1\ \mathrm{GeV}^2$.

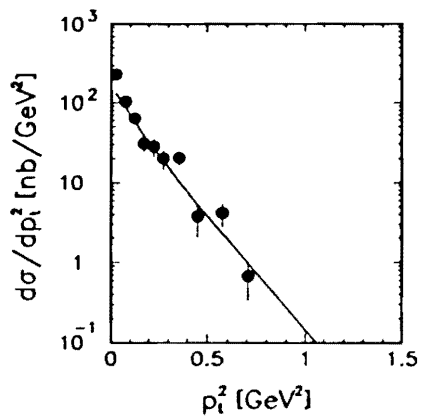

Figure 4: The differential cross section $d\sigma/dp_t^2$ for the deuteron at $Q^2 = 6\ \mathrm{GeV}^2$. The curve is the p_t^2 distribution predicted by the model of Ref. [10], in which exchange of two non-perturbative gluons was assumed. The curve was normalized to the data in the range $0.1 < p_t^2 < 1.0\,\mathrm{GeV}^2$.

The values of the ρ density matrix element r_{00}^{04} [17] measured in the EMC and NMC experiments are shown in Fig. 5 as a function of Q^2. This matrix element represents the probability that the produced ρ^0 is polarised longitudinally (helicity 0). The curves were calculated taking the ratio $R(Q^2)$ of the cross sections for exclusive ρ^0 production by longitudinal and transverse virtual photons as predicted by Ref. [10] and using the relation

$$r_{00}^{04} = \frac{\epsilon R}{1 + \epsilon R} \tag{4}$$

which is valid if the helicity in s-channel is conserved. In the above equation ϵ is the virtual photon polarisation. The solid line was calculated using values of ϵ for the NMC data, the dashed one - using the average ϵ for the EMC data. The large fractions of longitudinally polarised ρ^0 observed in both experiments are consistent with the model of Ref. [10], except for the lowest Q^2 data point. A similar prediction is given by the 'soft' pomeron model of Ref. [8].

The experimental data from muon experiments are not sufficient to prove s-channel helicity conservation (SCHC), which was observed to dominate the cross sections for exclusive ρ^0 production at small Q^2 [1]. However, the NMC data are consistent with the hypothesis of SCHC (decay azimuthal angular distributions, similarity of the measured r_{00}^{04} values for coherent and incoherent events) [4] and are in agreement with the models of Refs. [9-13] which predict either exact SCHC or dominant contribution of helicity conserving amplitudes.

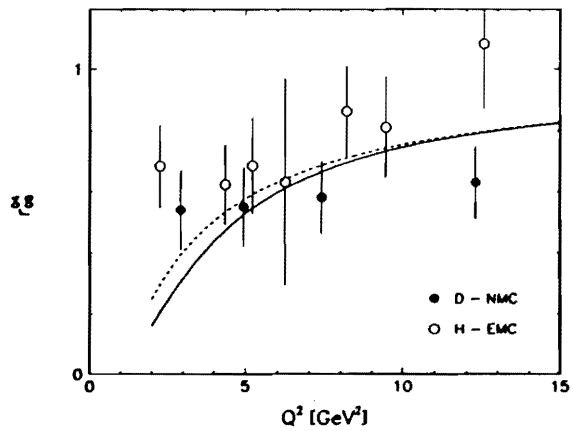

Figure 5: Fraction of ρ^0 mesons with helicity 0 (r^{04}_{00}) as a function of Q^2. The data are from the NMC [4] for the deuteron (full symbols) and from the EMC [2] for the proton (open symbols). The curves were obtained using predictions of the model of Ref. [10] for the NMC data (continuous line) and for the EMC data (dashed line). The difference between curves is due to the different virtual photon polarisations for both samples.

There are merely two experimental determinations of the ratio R for exclusive ρ^0 production at large Q^2. One is a direct determination of R by the EMC [2], $R = -.38 \pm 0.13^{+0.9}_{-0.4}$ at $Q^2 = 2$ GeV^2. This estimate has large errors due to the fact that the data from two different experiments were used to extrapolate the cross sections. Another is from the NMC experiment [4], $R = 2.0 \pm 0.3$ at $Q^2 = 6$ GeV^2. The latter was obtained assuming SCHC. At large Q^2 all models [8-13] predict large values of R and its linear growth with Q^2. For example, the model of Ref. [10] predicts R equal to about 0.4 at $Q^2 = 2$ GeV^2, and about 2 at $Q^2 = 6$ GeV^2. Within the errors both experimental estimates of R, each given at a different Q^2 value, are consistent with the predictions of this model.

In conclusion, the models assuming exchange of a pair of non-perturbative gluons fairly well reproduce all measured characteristics of the data from proton and deuteron targets in the kinematical range of the fixed target experiments. As discussed in Ref. [9] the 'soft' pomeron model give similar predictions.

3. The data from nuclear targets

In this section we compare the nuclear transparencies and the ratios of the p_t^2-integrated coherent cross sections for different nuclei with the colour transparency model predictions of ref. [12] and with predictions of the Glauber model in conjunction with the VMD model. The data are from the NMC [4] and the E665 [6] experiments. The E665 results are preliminary.

The nuclear transparency is defined as a ratio of the cross section per nucleon from a given nucleus to the cross section from a free nucleon in the range where coherent effects can be neglected. The nuclear transparencies as a function of Q^2 for carbon, calcium and lead are shown in Fig. 6. The E665 data extend to smaller Q^2

values than the NMC data, but in the range of overlap the two experiments agree.

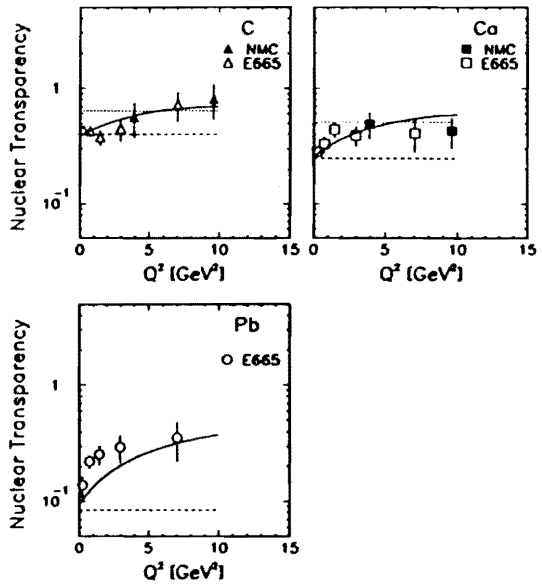

Figure 6: The Q^2 dependence of the nuclear transparency for incoherent exclusive ρ^0 virtual photoproduction. The data are from the NMC [4] (full symbols) and from the E665 [6] (open symbols). The solid curves are predictions of the colour transparency model [12]. The dotted and dashed lines are the Glauber-VMD model predictions described in the text.

The solid curves are predictions of the colour transparency model of Kopeliovich *et al.* [12] (KNNZ). The model reproduces the trend of the data i.e. increase of the nuclear transparency with increasing Q^2. The figure illustrates also that the regime of complete colour transparency (nuclear transparency ~ 1) is not attained yet at the presently accessible values of Q^2.

We further compare the measured nuclear transparencies to the predictions of the Glauber-VMD model. The predictions depend on the value of the coherence length $l_c = 2\nu/(Q^2 + m_\rho^2)$, which is the length of the path travelled by the virtual vector meson into which the virtual photon has fluctuated [1]. In the low- and high-coherence length limits one gets [18]

$$T_A^{Gl} = \frac{1}{A}\int d^2\mathbf{b}\{\frac{1-\exp[-\sigma_{tot}(\rho N)T(\mathbf{b})]}{\sigma_{tot}(\rho N)}\} \qquad (l_c < R_A), \tag{5}$$

$$T_A^{Gl} = \frac{1}{A}\int d^2\mathbf{b}T(\mathbf{b})\exp[-\sigma_{tot}(\rho N)T(\mathbf{b})] \qquad (l_c \gg R_A). \tag{6}$$

Here $T(\mathbf{b}) = \int_{-\infty}^{\infty} dz\, n_A(\mathbf{b}, z)$, $n_A(\mathbf{b}, z)$ is the nucleon density, $r = (\mathbf{b}, z)$ denotes the position of the photon absorption vertex, $\mathbf{b}$ is the impact parameter vector and R_A is the nuclear radius.

To calculate the nuclear transparencies, the nuclear densities were parametrised as in Ref. [19]. An estimate of the total cross section $\sigma(\rho^0 N)$ was obtained in the framework of the quark model [1], $\sigma(\rho^0 N) \approx \frac{1}{2}\{\sigma(\pi^+ p)+\sigma(\pi^- p)\}$, using high precision

measurements of the pion-proton total cross sections. From an interpolation of the pion-proton data [20] one obtains $\sigma(\rho^0 N) = 23.7 \pm 0.1$ mb at $\nu = 112$ GeV.

The nuclear transparencies predicted by the Glauber model are shown in Fig. 6 as the dotted and dashed lines for the case of small and large coherence length respectively. Because the NMC data cover the range where l_c is both below and above R_A ($R_C = 2.47$ fm, $R_{Ca} = 3.48$ fm), we show predictions of both formulae (5) and (6). The E665 data are more conclusive. They correspond to $l_c > R_A$ and should be compared to the dashed curves. Except for the lowest Q^2, the nuclear transparencies measured by E665 clearly disfavour the Glauber-VMD description.

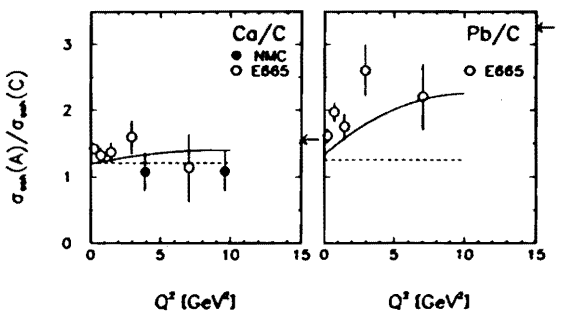

Figure 7: The Q^2 dependence of the ratio $\sigma^{Ca}_{coh}/\sigma^{C}_{coh}$ and $\sigma^{Pb}_{coh}/\sigma^{C}_{coh}$ (cross sections are given per nucleon) for coherent ρ^0 muoproduction. The data are from the NMC [4] (full symbols) and from the E665 [6] (open symbols). The solid curves are predictions of the colour transparency model [12]. The arrows indicate the predictions for complete colour transparency at $Q^2 \to \infty$. The dashed lines are the Glauber-VMD model predictions described in the text.

In Fig. 7 the ratios of p_t^2-integrated coherent cross sections $\sigma^{Ca}_{coh}/\sigma^{C}_{coh}$ and $\sigma^{Pb}_{coh}/\sigma^{C}_{coh}$ are shown. The continuous curves represent the colour transparency model (KNNZ) predictions. The arrows indicate the values expected at very large Q^2 for the complete colour transparency. The dashed curves correspond to the ratio of coherent cross sections predicted by the Glauber-VMD model, and given by the formula [12, 21]

$$\sigma^{A}_{coh} = \frac{1}{A} 4 \int d^2\mathbf{b}\{1 - \exp[-\frac{1}{2}\sigma_{tot}(\rho N)T(\mathbf{b})]\}^2. \tag{7}$$

This formula is obtained in the case when the longitudinal momentum transfer could be neglected (which is equivalent to $l_c \gg R_A$). For the numerical estimates the same value of the total cross section and the same parametrisations of nuclear densities were taken as for the incoherent nuclear transparency case discussed above.

The data for $\sigma^{Ca}_{coh}/\sigma^{C}_{coh}$ cannot discriminate between the two models. However, the preliminary E665 data on $\sigma^{Pb}_{coh}/\sigma^{C}_{coh}$ disfavour the Glauber-VMD description at larger Q^2.

In conclusion the nuclear effects for the exclusive ρ^0 production are fairy well reproduced by the colour transparency model of Ref. [12]. The nuclear absorption of the virtual quark-antiquark pair decreases with Q^2, but the regime of complete colour transparency is not attained yet. The Glauber-VMD description is disfavoured by the data, except at very small values of Q^2.

4. Conclusions

The data on exclusive ρ^0 production in deep inelastic muon scattering were compared with selected models. There is a fair agreement, essentially for all characteristics of the data from elementary targets (proton and deuteron), with the models which assume exchange of a pair of non-perturbative gluons. A similar agreement is obtained for the phenomenlogical 'soft' pomeron model. The nuclear effects seen for complex nuclei indicate that the nuclear absorption decreases with Q^2. This trend is reproduced by the colour transparency model of KNNZ. At large Q^2 the Vector Meson Dominance model has difficulties to describe simultaneously the Q^2 dependence of the cross sections and the large fractions of longitudinally polarised mesons. It predicts also, in conjunction with the Glauber model, a stronger nuclear absorption than observed for the data at large Q^2.

We consider possible extensions of the comparisons made in this paper to other models, in particular those using perturbative QCD approach, to be both interesting and important. We also emphasize the need for future comparisons to be comprehensive by taking into account all available measured characteristics.

References

[1] T.H. Bauer *et al.*, Rev. Mod. Phys. **50** (1978) 261.

[2] EMC, J.J.Aubert *et al.*, Phys. Lett. **B161** (1985) 203.

[3] EMC, J.Ashman *et al.*, Z. Phys. **C39** (1988) 169.

[4] NMC, M. Arneodo *et al.*, Nucl. Phys. **B429** (1994) 503.

[5] NMC, P. Amaudruz *et al.*, Z. Phys. **C54** (1992) 239.

[6] E665, G. Y. Fang, *in* Proceedings of Particle and Nuclei XIII International Conference, Perugia, Italy, 1993, editor A. Pascolini (World Scientific, Singapore, 1994) p.332; FERMILAB-Conf 93/305 (1993); private communication.

[7] ZEUS Collaboration, M. Derrick *et al.*, contributed paper ICHEP94 Ref. 0663 to the International Conference on High Energy Physics, Glasgow, 1994.

[8] A. Donnachie and P.V. Landshoff, Phys. Lett. **B185** (1987) 403.

[9] A. Donnachie and P.V. Landshoff, Nucl. Phys. **B311** (1989) 509;
P.V. Landshoff, Nucl.Phys. B (Proc.Suppl.) **18C** (1990) 211.

[10] J.R. Cudell, Nucl. Phys. **B336** (1990) 1.

[11] M.G. Ryskin, Z. Phys. **C57** (1993) 89.

[12] B.Z. Kopeliovich *et al.*, Phys. Lett. **B324** (1994) 469.

[13] S.J. Brodsky *et al.*, Phys. Rev. **50** (1994) 3134.

[14] B.Z.Kopeliovich *et al.*, Phys. Lett. **B309** (1993) 179.

[15] P.V. Landshoff, *in* Proceedings of Joint Lepton-Photon Symposium and Europhysics Conference on High Energy Physics, Geneva, 1991, editors S. Hegarty, K. Potter and E. Quercigh (World Scientific, Singapore, 1992) vol.2, p. 363.

[16] H. Fraas and D. Schildknecht, Nucl. Phys. **B14** (1969) 543.

[17] K. Schilling and G. Wolf, Nucl. Phys. **B 61** (1973) 381.

[18] N.N. Nikolaev, Int. J. Mod. Phys. E: Reports on Nucl. Phys. v.2, n.4 (1993).

[19] H. de Vries *et al.*, Atomic Data and Nucl. Data Tables **36** (1987) 495.

[20] V. Flaminio *et al.*, CERN-HERA 83-01 (1983).

[21] O. Benhar *et al.*, Phys. Rev. Lett. **69** (1992) 1156.